# A collection of restricted three-body test problems

P.W. Sharp
Department of Mathematics, University of Auckland, Private Bag 92019,
Auckland, NEW ZEALAND. sharp@scitec.auckland.ac.nz

March 27, 2001

**Abstract**

The restricted three-body problem has many important applications in astronomy. We present a collection of 20 problems and compare the popular integrators `ode45` and `ode113` from Matlab on the collection.

**MR Classification:** Primary - 65L06, secondary - 85-08

**Keywords:** Restricted three-body, collection, Matlab integrators

## 1 Introduction

The restricted three-body (R3B) problem has found many important astronomical applications since its formulation by Euler in 1772. It is used to model the orbits of celestial bodies including the Trojan asteroids and comets of Jupiter, the satellites Telesto, Calypso and Helene of Saturn, the interplanetary cloud in Earth's orbit and near Earth asteroids. It is also used to model the gamma-ray flux from binary star systems and the stability of barred galaxies, and to find orbits for spacecraft including lunar probes and robotic observatories. References for the applications include Abad, Arribas and Elipe [1], Bailyn, Garcia and Grindlay [2], Buccheri et. al. [3], van Houten and van Houten-Groneneveld [9], Kelsal et. al. [11], Oberti [13], Pfenniger [14], Taylor [20], Wiegart, Innanen and Mikkola [21], Zhang and Innanen [22, 23].

The R3B problem has two massive particles, the primaries, moving in circular orbits about their centre of mass and a massless particle moving in the plane of the primaries. Since the third particle is massless it does not interact with the primaries and their motion is described by the two-body problem. This problem can be solved analytically and the R3B problem reduces to finding the motion of the massless particle.

Euler and Lagrange found five periodic solutions to the R3B problem with the massless particle fixed relative to the primaries. These positions are called Lagrangian points and are depicted in Figure 1. Points $L_1$, $L_2$ and $L_3$ lie on the line of centres and $L_4$ and $L_5$ form equilateral triangles with the primaries.

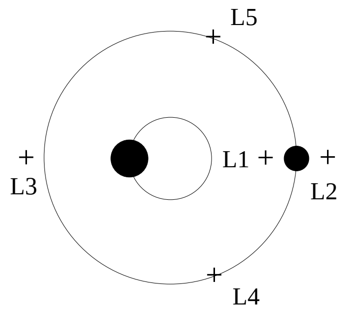


Figure 1: The + mark the five Lagrangian points.

These are the only non-trivial periodic solutions with the massless particle fixed relative to the primaries. If the massless particle need not be fixed, it is possible using numerical techniques to find an arbitrary number of periodic solutions. Darwin [4, 5] found solutions for $\mu = 1/11$ and Moulton [12] mostly for $\mu = 1/5$. From 1913 to 1939, a team led by Strömgrén [18] found families of solutions for mostly $\mu = 1/2$. Since the late 1950s there has been much interest in finding orbits for binary systems, particularly the Earth and Moon and the Sun and Jupiter. Szebehely [19] describes this work up to the mid 1960s and Hénon [8] more recent work.

The many applications of the R3B problem along with its simple specification means individual problems are commonly used to test integrators (see for example, [7] p 127, 197 and [10]). However there does not exist a collection of R3B problems for testing.

We present 20 problems and use them to compare the popular integrators `ode45` and `ode113` from Matlab. The problems vary according to the initial position of the massless particle on the $x$-axis and the number of loops in the orbit. There is more than a 30-fold variation in the periods. Small groups of the problems form sequences in which one parameter varies across the sequence. These sequences are intended to show trends in numerical performance. The problems model either the Earth and Moon or the Sun and Jupiter as primaries. We could have used other primaries but chose these because of the important applications involving them. The restriction to 20 problems is a pragmatic choice - many more problems and it becomes difficult to present the numerical results concisely and in sufficient detail.

In §2 we define the R3B problem and give the initial conditions and period for the 20 problems. We also discuss pertinent features of the problems. Then in §3 we present a summary of numerical comparisons between `ode45` and `ode113`. This summary covers the size of the global error, the percentage of failed steps and the efficiency.

# 2 Problems

We solve the R3B problem in a rotating rectangular Cartesian coordinates. The origin is at the centre of mass of the primaries and the $x$-axis is the line of centres. The units of distance, time and mass are chosen so the separation of the primaries is the unit distance, the period of rotation is $2\pi$ and the gravitational constant is one. Let $0 < \mu \leq 1/2$ denote the mass ratio of the lighter and heavier primaries. The equations of motion and initial conditions for the massless particle are (see for example, [15], p 126)

$$x'' = x + 2y' - (1-\mu)\frac{x - x_1}{r_1^3} - \mu\frac{x - x_2}{r_2^3}, \tag{1}$$

$$y'' = y - 2x' - (1-\mu)\frac{y}{r_1^3} - \mu\frac{y}{r_2^3}, \tag{2}$$

$$x(0) = x_0, \quad y(0) = 0, \quad x'(0) = 0, \quad y'(0) = y_0', \tag{3}$$

where $x_1 = -\mu$, $x_2 = 1 - \mu$, $r_1 = \sqrt{(x - x_1)^2 + y^2}$, $r_2 = \sqrt{(x - x_2)^2 + y^2}$ and without loss of generality, the initial conditions are at $t = 0$. The quantities $x_1$ and $x_2$ are the position on the $x$-axis of the primaries of mass $1 - \mu$ and $\mu$ respectively, and $r_1$ and $r_2$ are the distances of the massless particle from the primaries.

Table 1 gives $x(0)$, $y'(0)$ and the period $T$ for our 20 problems[1]. Plots of the phase plane and the velocity are in the Appendix. The values of $x(0)$ are exact while $y'(0)$ and $T$ are correct to 20 significant figures and are either published results or were calculated in quadruple precision using simple shooting and continuation. By accurate to 20 significant figures, we mean the values were found to more than 20 significant figures and then rounded. For conciseness, we refer to Problem i, $1 \leq \text{i} \leq 20$, as Pi.

The last two columns of Table 1 give the number of steps $N$ and the average stepsize $\bar{h}$ used by `ode45` for mixed relative and absolute tolerances of $10^{-10}$. $N$ and $\bar{h}$ are presented as simple measures of the effort required to solve the problems. We chose tolerances of $10^{-10}$ to ensure the true orbit was followed closely and there were few failed steps. `ode45` performed very well in the latter regard, having just two failed steps, one each on P17 and P18, out of 38,053 attempted steps. We observe from Table 1 that there is a 6-fold variation in $N$ and a 14-fold variation in $\bar{h}$ across the 20 problems.

P1 to P15 have $\mu = 0.012277471$ and model the Earth and Moon as the primaries. The Earth is at $(-0.012277471, 0)$ and the Moon at $(0.987722529, 0)$. P16 to P20 have $\mu = 0.000953875$ and model the Sun and Jupiter as the primaries. The Sun is at $(-0.000953875, 0)$ and Jupiter at $(0.999046125, 0)$.

P1 to P3 are possibly the most common R3B problems in the numerical literature. They have $x(0) = 0.994$ and form a sequence with the number of loops in the orbit increasing by one with consecutive problems. The values of $x(0)$ and $T$ for P1 were found by refining the values on page 246 of [17]; $x(0)$ and $T$ for P2 and P3 were taken from pages 200 and 128 of [7]. $T$ and $N$ increase with the problem index, but the relative increase in $N$ is less than that for $T$ and $\bar{h}$ increases with the index.

P4 has one more loop and $x(0)$ 0.003 larger than P3. P4, taken with P1 to P3, illustrate how the numerical performance can depend on the number of loops and the distance of closest approach to the Moon.

P5 to P7 have $x(0) = 0.869972$ and form a sequence with the number of loops increasing by two with consecutive problems. P5 to P7 are unusual in that the massless particle

[1] The table is available at `http://www.scitec.auckland.ac.nz/~sharp/r3b_20sf.html`

| | $x(0)$ | $y'(0)$ | $T$ | $N$ | $10^3\bar{h}$ |
|---|---|---|---|---|---|
| 1 | 0.994000E+00 | -0.21138987966945026683E+01 | 0.54367954392601899690E+01 | 865 | 6.3 |
| 2 | 0.994000E+00 | -0.20317326295573368357E+01 | 0.11124340337266085135E+02 | 961 | 11.6 |
| 3 | 0.994000E+00 | -0.20015851063790825224E+01 | 0.17065216560157962559E+02 | 1071 | 15.9 |
| 4 | 0.997000E+00 | -0.16251217072210773125E+01 | 0.22929723423442969481E+02 | 1067 | 21.5 |
| 5 | 0.879962E+00 | -0.66647197988564140807E+00 | 0.63006757422352314657E+01 | 1198 | 5.3 |
| 6 | 0.879962E+00 | -0.43965281709207999128E+00 | 0.12729711861022426544E+02 | 1358 | 9.4 |
| 7 | 0.879962E+00 | -0.38089067106386964470E+00 | 0.19138746281183026809E+02 | 1682 | 11.4 |
| 8 | 0.997000E+00 | -0.18445010489730401177E+01 | 0.12353901248612092736E+02 | 2139 | 14.4 |
| 9 | 0.100000E+01 | -0.16018768253456252603E+01 | 0.12294387796695023304E+02 | 1880 | 6.5 |
| 10 | 0.100300E+01 | -0.14465123738451062297E+01 | 0.12267904265603897140E+02 | 1769 | 6.9 |
| 11 | 0.120000E+01 | -0.71407169828407848921E+00 | 0.18337451820715063383E+02 | 1039 | 17.6 |
| 12 | 0.120000E+01 | -0.67985320356540547720E+00 | 0.30753758552146029263E+02 | 1501 | 20.5 |
| 13 | 0.120000E+01 | -0.67153130632829144331E+00 | 0.43214375227857454128E+02 | 1991 | 21.7 |
| 14 | 0.120000E+01 | -0.66998291305226832207E+00 | 0.55672334134347612727E+02 | 2494 | 22.3 |
| 15 | 0.120000E+01 | -0.66975741517271092087E+00 | 0.68127906604713772763E+02 | 2999 | 22.7 |
| 16 | -0.102745E+01 | 0.40334488290490413053E−01 | 0.18371316400018903965E+03 | 2422 | 75.8 |
| 17 | -0.976680E+00 | -0.61191623926410837000E−01 | 0.17733241131524483004E+03 | 3334 | 53.2 |
| 18 | -0.766650E+00 | -0.51230158665978820282E+00 | 0.17660722897242937108E+03 | 5238 | 33.7 |
| 19 | -0.109137E+01 | 0.14301959822238380020E+00 | 0.82949461922342093092E+02 | 1659 | 50.0 |
| 20 | -0.110137E+01 | 0.15354250908611454510E+00 | 0.60952121909407746612E+02 | 1384 | 44.0 |

Table 1: The initial conditions $x(0)$, $y'(0)$, period $T$, number of steps $N$ and average stepsize $\bar{h}$ for the 20 problems. $N$ and $\bar{h}$ are for `ode45` with a tolerance of $10^{-10}$.

orbits just one of the primaries, the Earth in this case. The initial conditions and period for P7 were supplied to eight decimal places by Butcher [private communication]. As with P1 to P3, $\bar{h}$ increases with the problem index.

P8 to P10 are sometimes called bus orbits and form a sequence with increasing $x(0)$. In each orbit, the massless particle, representing a lunar probe, makes four flybys of the Earth, and two of the Moon, one each on the near and far sides of the Moon. The closer $x(0)$ is to the Moon, the closer all six flybys are to the primaries. Figure 2 gives the phase plane and velocity for P8. The four large spikes in the velocity occur during the terrestial flybys and the two small spikes, at $t = 0$ and near $t = 6$, occur during the lunar flybys. The plots for P9 and P10 are similar except the flybys are further from the primaries and the velocity spikes smaller.

To accurately integrate the flybys, an integrator must reduce the stepsize markedly from the values used far from the primaries. The bottom plot of Figure 2 gives the stepsizes used by `ode45` on P8 for mixed relative and absolute tolerances of $10^{-10}$. The ratio of the largest to smallest stepsize is 534.

P11 to P15 have $x(0) = 1.2$ and form a sequence with the number of loops increasing by two with consecutive problems. The period increases almost linearly with the problem index and there is only a small variation in $\bar{h}$.

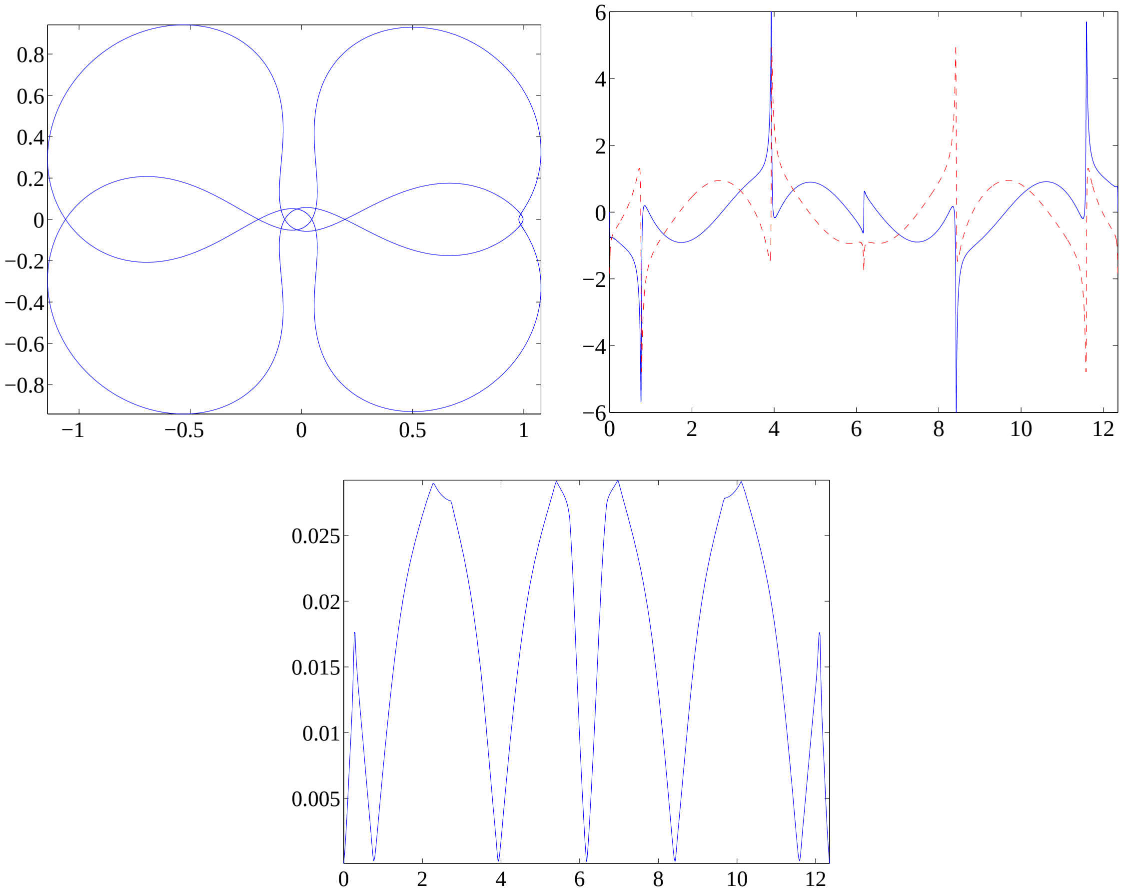


Figure 2: Plots for P8. Top left - phase plane, top right - $x'(t)$ (–), $y'(t)$ (- -), bottom - the stepsize as a function of time for `ode45` with mixed relative and absolute tolerances of $10^{-10}$.

P16 to P20 are horseshoe orbits that encircle $L_3$, $L_4$ and $L_5$. The initial conditions and period for P16 to P18 were found by refining the values given for orbits b, c and d in Table 1 of [20]. P19 and P20 were suggested by orbits c and d in Figure 4 of [20]. The average stepsize $\bar{h}$ for P16 to P20 is noticeably larger than for P1 to P15, suggesting P16 to P20 require fewer derivative evaluations at severe tolerances. The phase plane plot for P16 is a smooth horseshoe to plotting resolution. However, $x'(t)$ and $y'(t)$ have small oscillations in the middle part of the orbit. These are a precursor to the 28 loops of P17.

# 3 Comparisons of ode45 and ode113

`ode45` is a variable-stepsize method based on a 4-5 explicit Runge-Kutta pair and `ode113` is a variable-order, variable-stepsize Adams method. `ode45` requires seven derivative evaluations on the first step and six on all others; `ode113` requires two derivative evaluations on accepted steps and one on failed steps.

We solved P1 to P20 using `ode45` and `ode113` for mixed relative and absolute tolerances of $10^{-j}$, $j = 2, \ldots, 10$. Below is a summary of the numerical results. All calculations were performed in Matlab 5.3, on a single processor of a SGI Origin 2000.

Table 2 gives $\log_{10} ||E||_2$ for `ode45`, where $E$ is the global error after one period and is defined as $[x_n(T) - x(0), y_n(T) - y(0), x'_n(T) - x'(0), y'_n(T) - y'(0)]^T$, the subscript $n$ denoting the numerical solution.

We observe from Table 2 that $||E||_2$ is not less than one for all problems until the tolerance is decreased to $10^{-6}$. This observation confirms an earlier one of Shampine [16]. Shampine found that when `ode45` is used with the default tolerance of $10^{-3}$ to solve the R3B problem supplied with Matlab, the global error is appreciable.

`ode113` fared no better than `ode45`, failing on P8 and P14 with a tolerance of $10^{-2}$. `ode113` stopped the integration of P8 at $t = 0.804T$ because it was unable to meet the integration tolerance without reducing the step size below the smallest value allowed of $3.5 \times 10^{-14}$. The reason was the same for P14, except the time was $0.444T$ and the stepsize $8.7 \times 10^{-14}$.

`ode45` found a more accurate solution than `ode113` for most problems and tolerances, but as discussed later in this section, this was at the expense of more derivative evaluations. P8, P9, P10 and P18 had the largest global errors at severe tolerances.

An important measure of an integrator is the number of failed steps. Table 3 gives the ratios $R_m$, $R_a$ and $R_M$. These are defined as

$$R_m = 100 \min_i \left\{ \frac{n^f_{ij}}{n^a_{ij}} \right\}, \quad R_a = \frac{100}{20} \sum_{i=1}^{20} \frac{n^f_{ij}}{n^a_{ij}}, \quad R_M = 100 \max_i \left\{ \frac{n^f_{ij}}{n^a_{ij}} \right\},$$

where $n^f_{ij}$ and $n^a_{ij}$ are the number of failed and accepted steps respectively for problem Pi and tolerance $10^{-j}$. $R_m$, $R_a$ and $R_M$ are the minimum, average and maximum percentage respectively of failed steps over the 20 problems for one tolerance. When calculating these ratios for `ode113`, we omitted P8 and P14 for the tolerance $10^{-2}$.

The ratios for both integrators decrease monotonically with the tolerance, except for `ode45` with a tolerance of $10^{-4}$. This monotonicity is expected from the error expansion of the local error estimate. There is a marked difference between the two integrators. At a tolerance of $10^{-2}$, the ratios for `ode45` are several times larger than for `ode113`. As the tolerance decreases the ratios for `ode45` decrease faster than for `ode113` and for tolerances of $10^{-7}$ and less, the ratios for `ode45` are smaller.

Our final comparison is of the number of derivative evaluations required to achieve a prescribed global error. We found `ode113` was more efficient than `ode45` at small tolerances. This was expected because `ode113` uses high orders for small tolerances. At large tolerances, the integrators were of comparable efficiency. This was a little unexpected. We thought since `ode113` uses lower orders at large tolerances than at small tolerances, `ode45` may have been more efficient. However, this expectation does not allow for the higher percentage of failed steps by `ode45` at large tolerances.

Figure 3 contains two log-log plots of the number of derivative evaluations against $||E||_2$. The left plot is for P6 and the right for P16. These two plots are representative of the range in the relative efficiency of `ode45` and `ode113` on the 20 problems.

| | Problems | | | | | | | | | | | | | | | | | | | |
|---|---|---|---|---|---|---|---|---|---|---|---|---|---|---|---|---|---|---|---|---|
| | 1 | 2 | 3 | 4 | 5 | 6 | 7 | 8 | 9 | 10 | 11 | 12 | 13 | 14 | 15 | 16 | 17 | 18 | 19 | 20 |
| - 2 | 0.4 | 0.3 | 0.3 | 0.3 | 1.6 | 0.0 | 0.5 | 1.9 | 0.0 | 0.2 | 0.1 | 0.1 | 0.7 | 0.1 | 1.1 | 2.2 | 2.2 | 0.1 | 0.2 | -0.5 |
| - 3 | -0.2 | 0.4 | 0.3 | 0.0 | -0.7 | -0.5 | -0.4 | 0.1 | 0.0 | -0.1 | -1.5 | -0.7 | -1.4 | 0.2 | 0.1 | -0.6 | 0.2 | 0.4 | 0.3 | -0.9 |
| - 4 | -0.1 | -0.3 | -0.5 | -1.3 | -1.2 | -1.0 | -1.0 | 0.6 | 0.1 | 0.2 | -2.0 | -1.5 | -1.0 | 0.2 | 0.2 | -2.8 | -0.8 | 0.2 | -1.8 | -1.9 |
| - 5 | -1.1 | -0.9 | -1.1 | -2.0 | -2.4 | -2.0 | -2.0 | 0.0 | -0.1 | -0.1 | -2.7 | -2.2 | -1.6 | -1.1 | 0.2 | -3.4 | -1.2 | -0.2 | -4.0 | -2.3 |
| - 6 | -2.8 | -2.5 | -2.8 | -3.0 | -3.8 | -3.5 | -3.5 | -0.6 | -2.4 | -1.7 | -4.2 | -3.9 | -3.3 | -2.5 | -1.7 | -4.2 | -2.3 | -0.3 | -4.3 | -3.2 |
| - 7 | -3.7 | -3.7 | -3.3 | -3.8 | -5.7 | -6.3 | -5.2 | -1.3 | -1.5 | -1.7 | -5.8 | -5.0 | -4.4 | -3.6 | -2.7 | -5.4 | -3.4 | -1.2 | -5.0 | -4.0 |
| - 8 | -4.6 | -4.4 | -4.1 | -4.8 | -6.3 | -5.9 | -5.7 | -2.1 | -2.4 | -2.6 | -6.4 | -5.7 | -5.1 | -4.3 | -3.4 | -6.6 | -4.4 | -2.3 | -5.8 | -5.0 |
| - 9 | -5.5 | -5.3 | -5.1 | -5.7 | -7.1 | -6.8 | -6.6 | -3.1 | -3.4 | -3.7 | -7.2 | -6.7 | -6.0 | -5.2 | -4.4 | -7.7 | -5.5 | -3.4 | -6.7 | -6.0 |
| -10 | -6.5 | -6.2 | -6.0 | -6.7 | -8.1 | -7.7 | -7.5 | -4.1 | -4.5 | -4.7 | -8.2 | -7.6 | -7.0 | -6.2 | -5.3 | -8.8 | -6.5 | -4.4 | -7.7 | -7.1 |

| | Problems | | | | | | | | | | | | | | | | | | | |
|---|---|---|---|---|---|---|---|---|---|---|---|---|---|---|---|---|---|---|---|---|
| | 1 | 2 | 3 | 4 | 5 | 6 | 7 | 8 | 9 | 10 | 11 | 12 | 13 | 14 | 15 | 16 | 17 | 18 | 19 | 20 |
| - 2 | 0.1 | 0.3 | 0.3 | 0.3 | 0.5 | 0.4 | 0.2 | ** | 0.7 | 0.6 | 0.3 | 1.0 | 0.8 | ** | 0.6 | 0.0 | -0.1 | 0.2 | 0.9 | 0.2 |
| - 3 | 0.2 | 0.3 | 0.2 | 0.2 | -0.1 | 0.2 | -0.3 | 1.0 | 0.3 | 0.1 | -0.4 | 0.0 | 0.2 | 1.5 | 1.4 | -0.5 | 0.0 | 0.3 | -0.3 | 0.0 |
| - 4 | 0.0 | 0.0 | -0.1 | -0.2 | -0.9 | -0.7 | -1.3 | 0.0 | -0.1 | 0.2 | -1.3 | -1.4 | 0.0 | 1.1 | 0.6 | -1.7 | 0.0 | -0.1 | -0.3 | 0.0 |
| - 5 | -0.6 | -0.7 | -1.1 | -1.3 | -1.6 | -2.0 | -2.8 | 0.3 | -0.1 | -0.1 | -2.6 | -2.5 | -1.4 | -1.2 | 0.1 | -3.3 | -1.3 | 0.5 | -1.6 | -0.4 |
| - 6 | -2.3 | -2.4 | -1.8 | -2.7 | -3.7 | -3.1 | -3.8 | -0.2 | -0.1 | -0.2 | -4.4 | -3.0 | -2.5 | -1.7 | -0.8 | -4.5 | -2.2 | 0.0 | -2.8 | -1.3 |
| - 7 | -2.4 | -2.9 | -2.9 | -3.7 | -4.2 | -4.0 | -4.4 | -0.4 | -1.1 | -0.8 | -5.4 | -4.9 | -3.6 | -3.2 | -2.2 | -5.2 | -3.2 | -0.3 | -3.5 | -3.3 |
| - 8 | -4.2 | -3.6 | -3.9 | -4.0 | -4.9 | -5.0 | -6.3 | -1.5 | -1.5 | -1.9 | -5.7 | -4.9 | -4.6 | -3.5 | -2.8 | -5.7 | -4.6 | -1.7 | -4.2 | -3.6 |
| - 9 | -4.5 | -4.9 | -4.7 | -5.2 | -6.3 | -6.1 | -6.1 | -1.9 | -2.7 | -3.1 | -6.7 | -6.2 | -5.7 | -4.5 | -4.8 | -7.0 | -4.8 | -3.0 | -5.2 | -4.4 |
| -10 | -6.2 | -5.3 | -6.0 | -6.2 | -7.5 | -7.4 | -7.0 | -3.1 | -4.6 | -3.9 | -7.4 | -7.0 | -6.2 | -5.6 | -4.7 | -7.5 | -6.2 | -3.3 | -7.1 | -5.8 |

Table 2: $\log_{10} ||E||_2$ for `ode45` (top) and `ode113` (bottom). The left most column is the base-10 logarithm of the tolerance. An entry of ** means the integration failed.

# References


[1] A. Abad, M. Arribas, A. Elipe, *On the attitude of a spacecraft near a Lagrangian point*, Bull. Astron. Inst. Czechosl. **40**, (1989), 302-307.

[2] C.D. Bailyn, M.R. Garcia, J.E. Grindlay, *Outflow from the outer Lagrangian point: observations and models of 4U 2127+12 in M15*, Astrophy. J., **344** (1989), 786-790.

[3] R. Buccheri, V. Salamone, K. Bennett, M. Busetta, L. Kuiper, W. Hermsen, M. McConnell, R. Much, J. Ryan, V. Schönfelder, H. Steinle, *Search for gamma-ray emission from the Lagrangian points of PSR 1957+20*, Astron. Astrophys. Suppl. Ser., **115** (1996), 305-309.

[4] G.H. Darwin, *Periodic Orbits*, Acta Math., **21** (1897), 99 - 242.

[5] G.H. Darwin, *On certain families of periodic orbits*, Mon. Not. Roy. Astr. Soc., **70** (1909), 108 - 143.

| | | Tolerances | | | | | | | | |
|---|---|---|---|---|---|---|---|---|---|---|
| | | $10^{-2}$ | $10^{-3}$ | $10^{-4}$ | $10^{-5}$ | $10^{-6}$ | $10^{-7}$ | $10^{-8}$ | $10^{-9}$ | $10^{-10}$ |
| `ode45` | $R_m$ | 4.2 | 2.9 | 2.8 | 0.6 | 0 | 0 | 0 | 0 | 0 |
| `ode113` | $R_m$ | 1.9 | 0.3 | 0.2 | 0 | 0 | 0 | 0 | 0 | 0 |
| `ode45` | $R_a$ | 26.4 | 23.1 | 20.0 | 11.6 | 4.5 | 0.8 | 0.1 | 0.1 | 0.0 |
| `ode113` | $R_a$ | 7.0 | 6.2 | 5.5 | 4.4 | 3.3 | 2.7 | 2.2 | 1.9 | 1.4 |
| `ode45` | $R_M$ | 47.3 | 34.4 | 37.9 | 30.2 | 13.3 | 2.5 | 0.4 | 0.2 | 0.1 |
| `ode113` | $R_M$ | 11.3 | 9.3 | 8.9 | 7.6 | 5.5 | 4.3 | 3.5 | 3.1 | 2.2 |

Table 3: The percentage of failed steps.

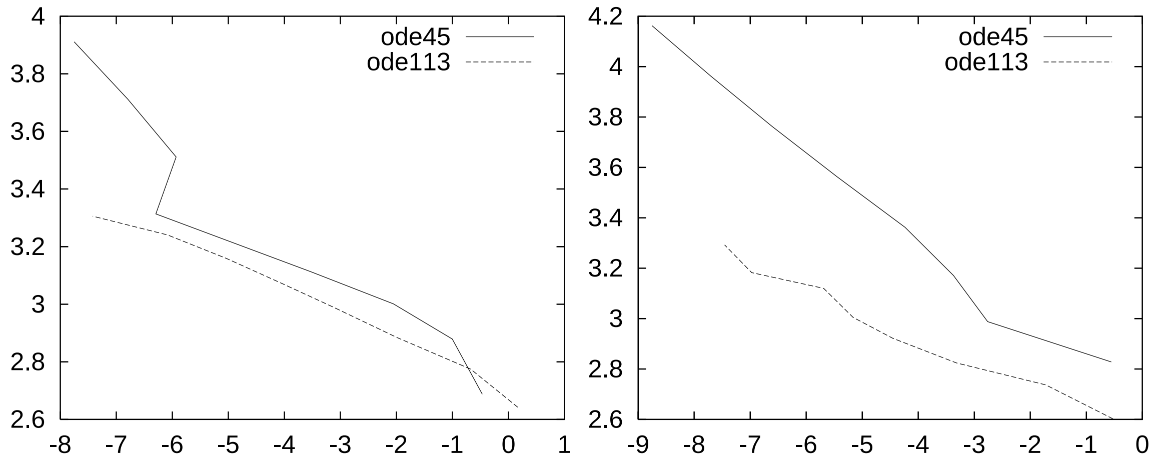


Figure 3: Base 10 log-log plots of the number of derivative evaluations (vertical) against $||E||_2$. Left - P6, right - P16.


[6] G.A. Gurzadyan, *Theory of interplanetary flights*, Overseas Publishers Association, Amsterdam, 1996.

[7] E. Hairer, S.P. Nørsett, G. Wanner, *Solving ordinary differential equations I: nonstiff problems*, Springer-Verlag, Berlin, 1987.

[8] M. Hénon, *Generating families in the restricted three-body problems*, Lecture notes in Physics 52, Springer Verlag, 1997.

[9] C.J. van Houten, I. van Houten-Groeneveld, *Minor planets and related objects. V. The density of Trojans near the preceding Lagrangian point*, Astron. J., **75** (1970), 5, 659 - 662.

[10] Tian-Yi Huang, K. Innanen, *A survey of multiderivative multistep integrators*, Astron. J., **112** (1996), 3, 1254-1262.

[11] T. Kelsall, J.L. Weiland, B.A. Franz, W.T. Reach, R.G. Arendt, E. Dwek, H.T. Freudenreich, M.G. Hauser, S.H. Moseley, N.P. Odegard, R.F. Silverberg, E.L. Wright, *The COBE diffuse infrared background experiment search for the cosmic infrared background. II. Model of the interplanetary dust cloud*, Astrophy. J., **508** (1998), 44-73.

[12] F.R. Moulton, *Periodic orbits*, Carnegie Inst., Washington, 1920.

[13] P. Oberti, *Lagrangian satellites of Tethys and Dione: II. theory of motion*, Astron. Astrophys., **228** (1990), 275-283.

[14] D. Pfenniger, *Stability of the Lagrangian points in stellar bars*, Astron. Astrophys., **230** (1990), 55-66.

[15] A.E. Roy, *Orbital motion*, 1ed, Adam Hilger, Bristol, 1978.

[16] L.F. Shampine, *Conservation laws and the numerical solution of ODEs II*, to appear in Comp. & Maths. with Appl.

[17] L.F. Shampine, M.K. Gordon, *Computer solution of ordinary differential equations: the initial value problem*, W.H. Freeman, San Francisco, 1975.

[18] E. Strömgrén, *Symmetrische und unsymmetrische librationsähnliche Bahnen in Problem Restreint mit asymptotisch-peridischen Bahnen als Grenzbahnen*, Copenhagen Obs. Publ., **97**, 1934.

[19] V. Szebehely, *Theory of orbits*, Academic Press, New York, 1967.

[20] D.B. Taylor, *Horseshoe periodic orbits in the restricted problem of three bodies for a Sun-Jupiter mass ratio*, Astron. Astrophys., **103** (1981), 288-294.

[21] P. Wiegert, K. Innanen, S. Mikkola, *The orbital evolution of near-Earth asteroid 3753 (1986 TO)*, American Astronomical Society, DPS meeting 29, July 1997.

[22] S.-P. Zhang, K.A. Innanen, *A numerical investigation of the stability of Saturn's triangular Lagrange points*, Astron. J., **96** (1988), 6, 1983 - 1988.

[23] S.-P. Zhang, K.A. Innanen, *A numerical investigation of the stability of the triangular Lagrange points of the planets*, Astron. J., **96** (1988), 6, 1989 - 1994.

# Appendix

The plots below give the phase plane, $x'(t)$ and $y'(t)$ for P1 to P20, excluding P8 for which the plots are in §2. The two plots for each problem are arranged horizontally with the phase plane on the left and the velocity components on the right, with $x'(t)$ and $y'(t)$ represented by a solid and dashed line respectively.

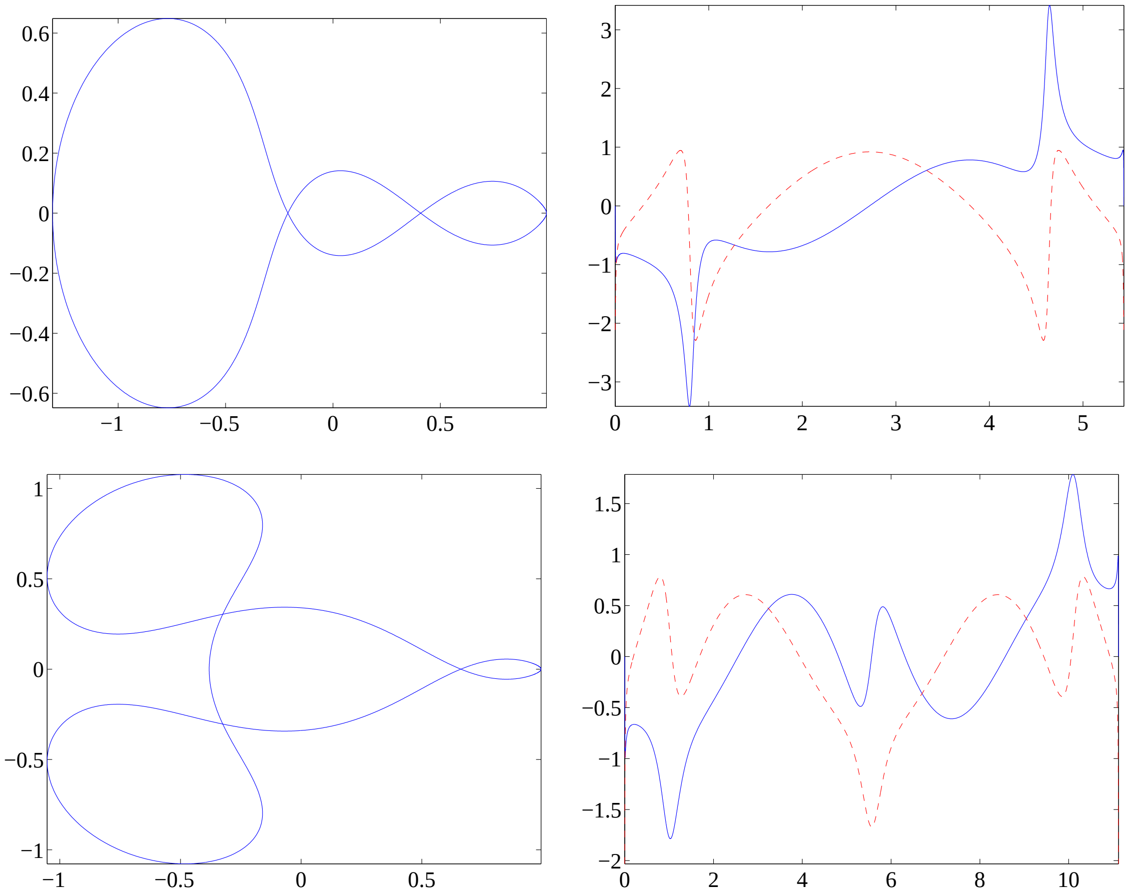


Figure 4: P1 (top), P2 (bottom).

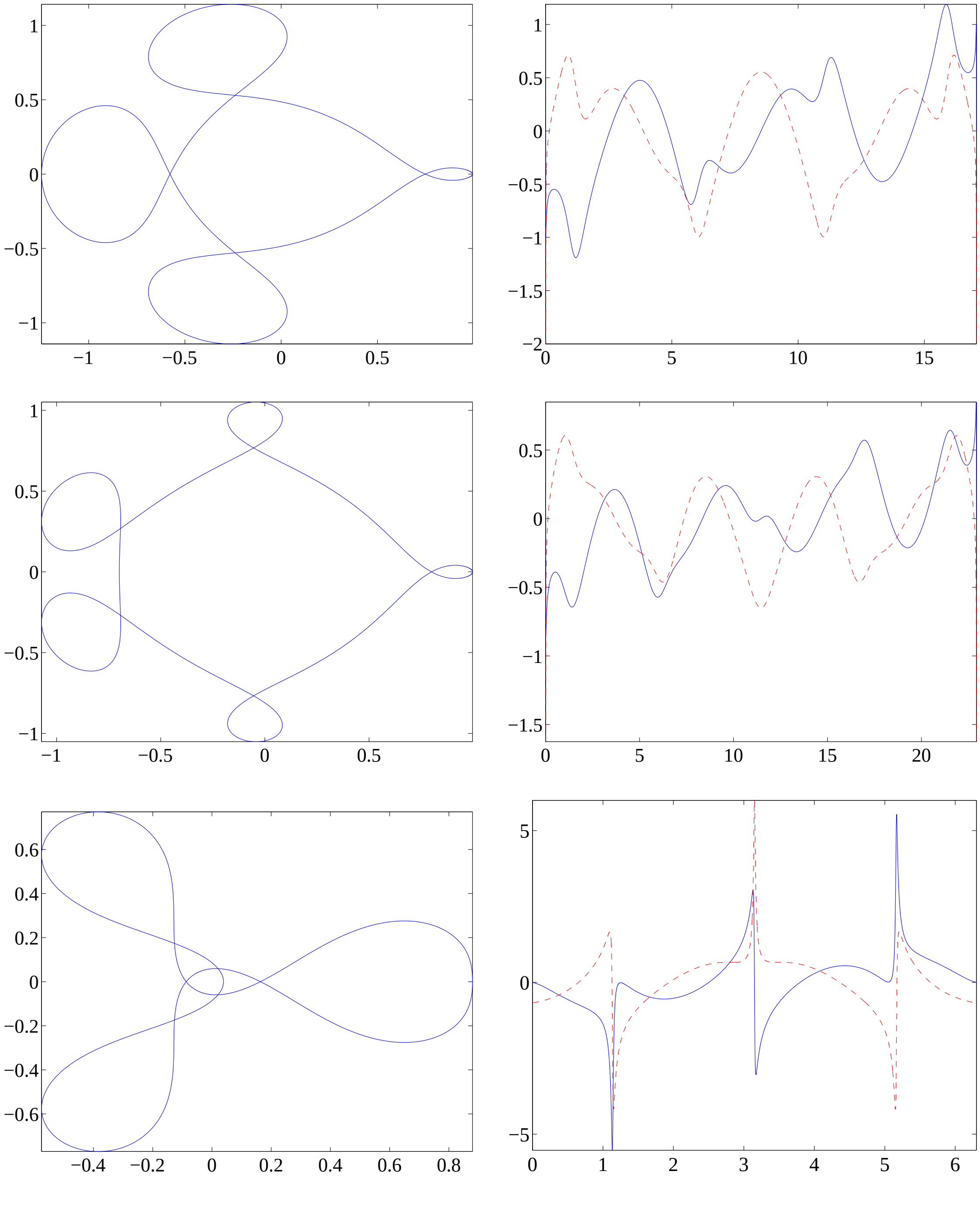

Figure 5: P3 (top), P4 (middle), P5 (bottom).

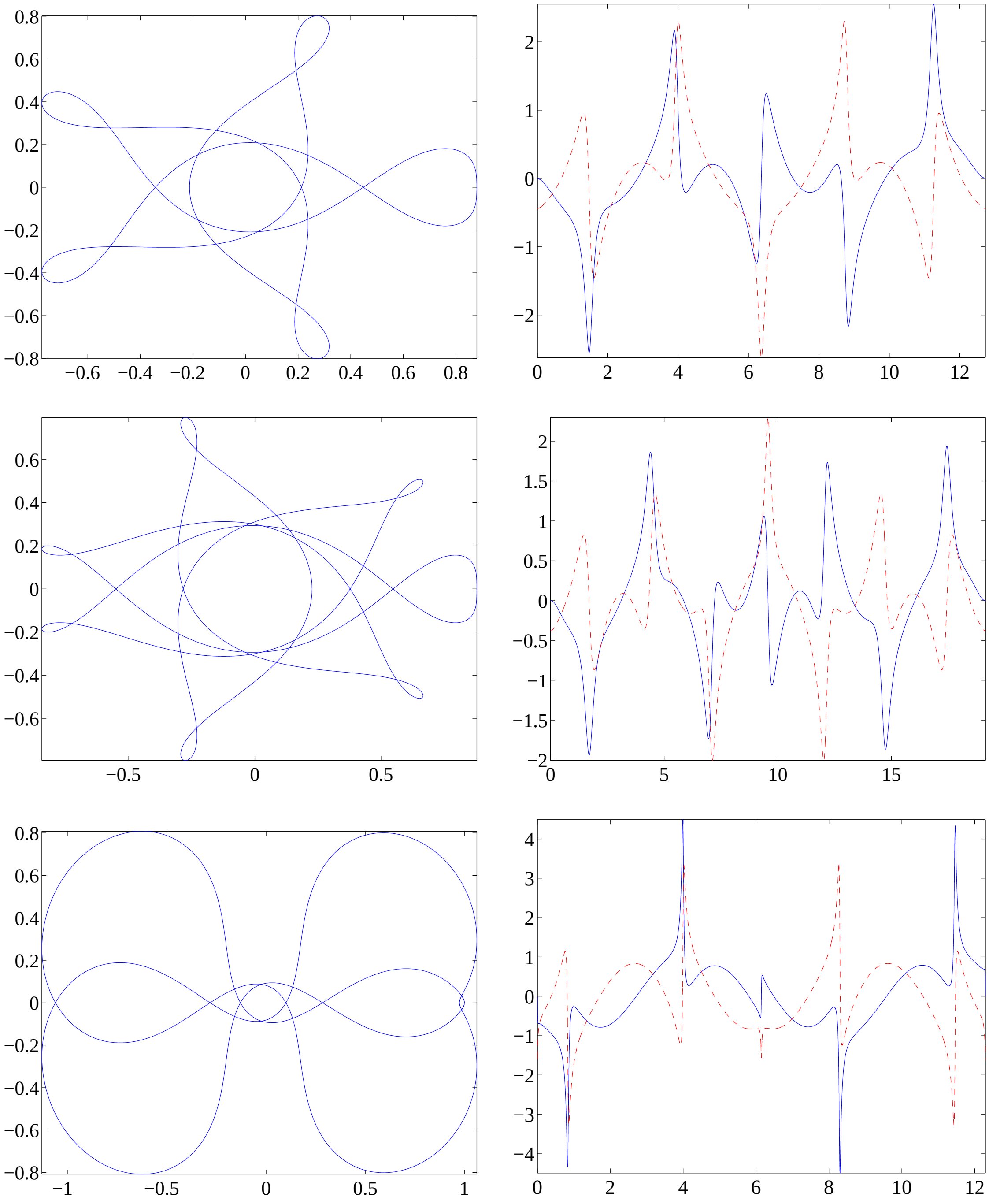


Figure 6: P6 (top), P7 (middle), P9 (bottom).

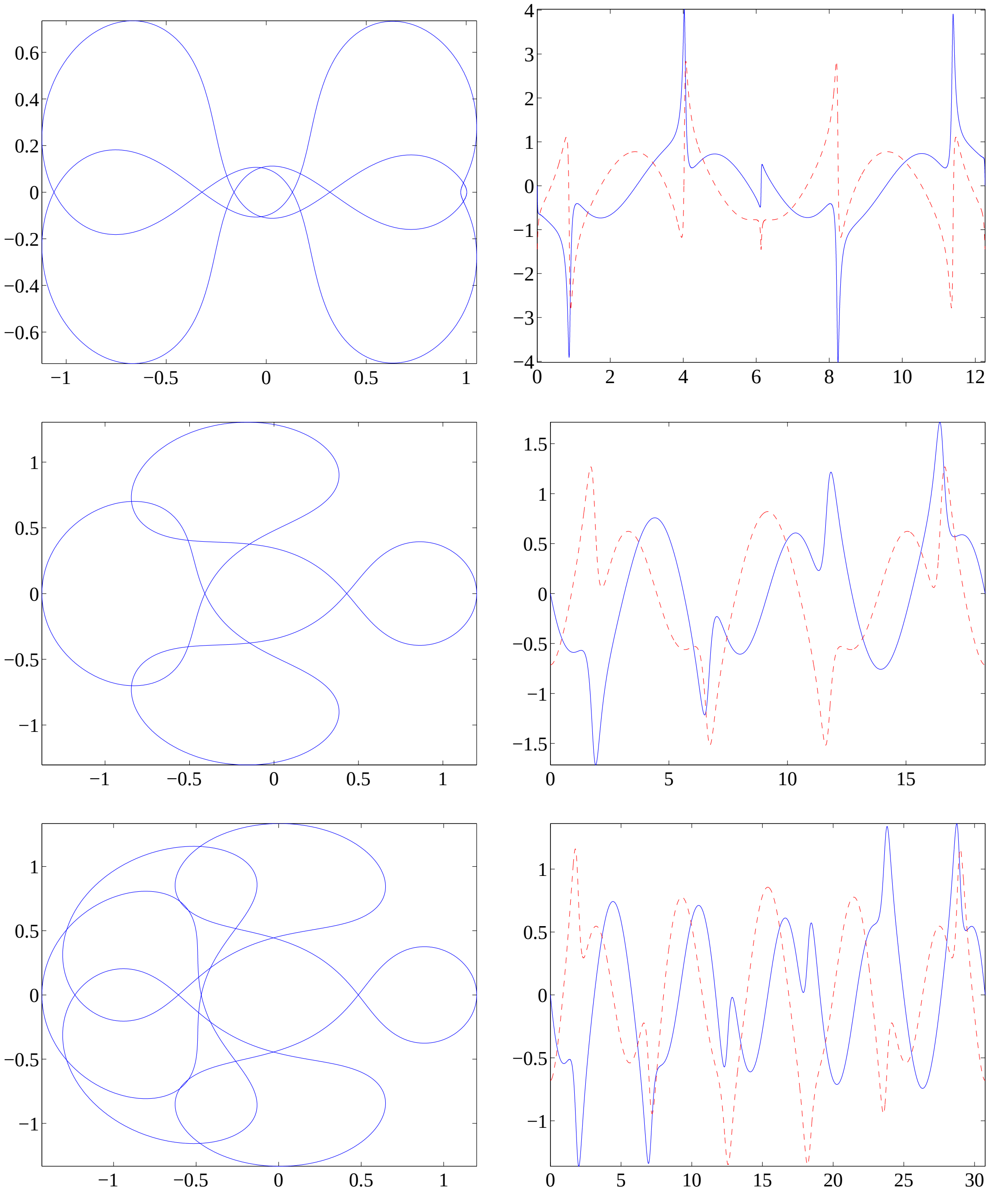


Figure 7: P10 (top), P11 (middle), P12 (bottom).

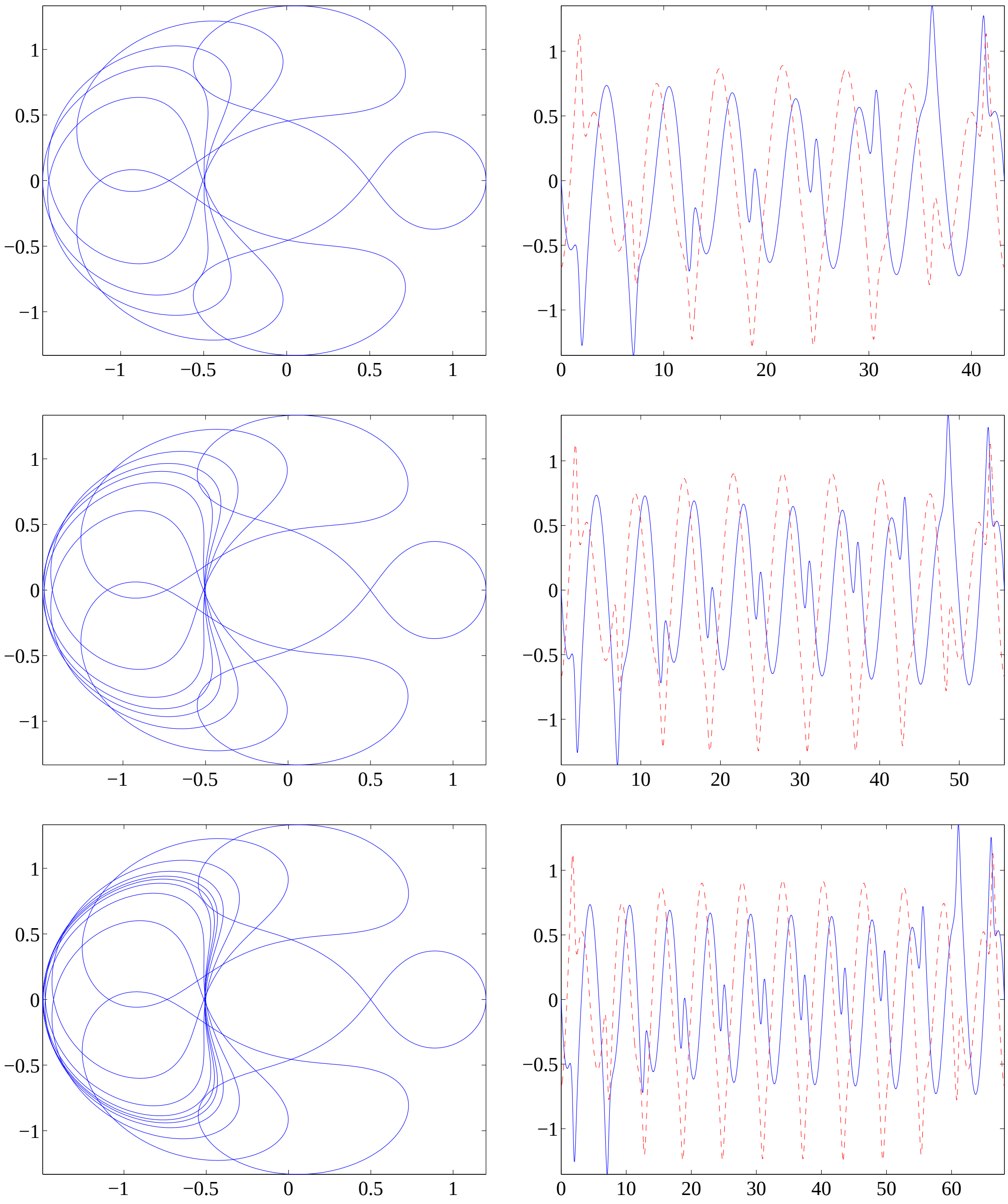

Figure 8: P13 (top), P14 (middle), P15 (bottom).

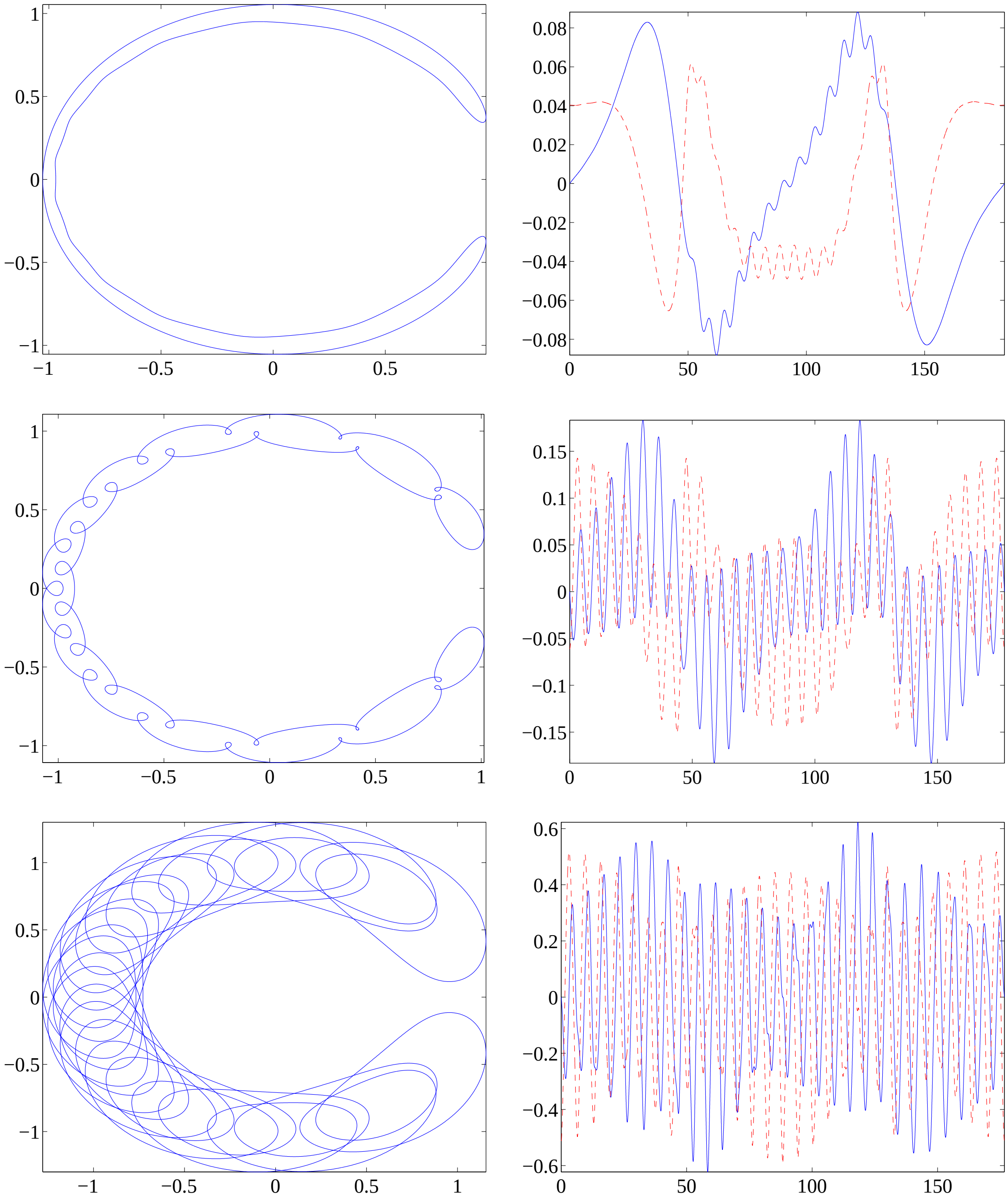


Figure 9: P16 (top), P17 (middle), P18 (bottom).

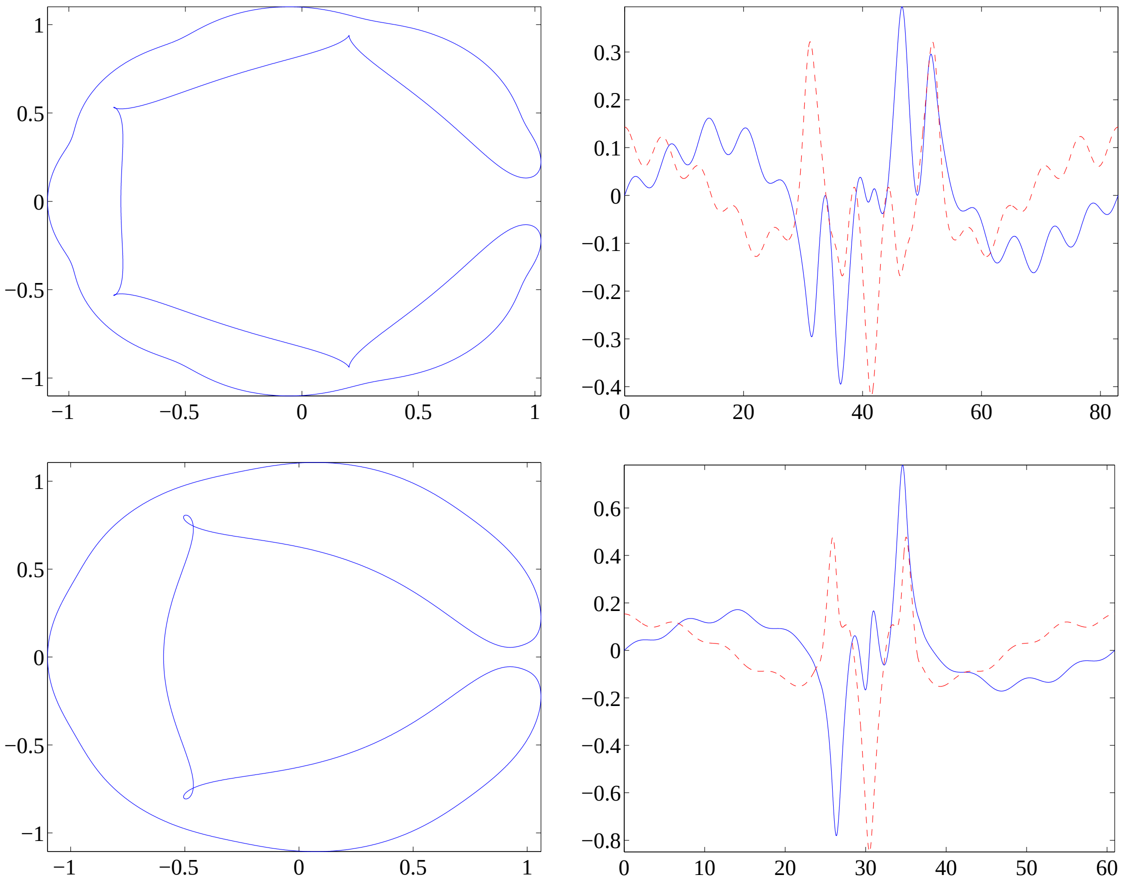


Figure 10: P19 (top) and P20 (bottom).